Algerian Journal of Chemical Engineering
ISSN: 2773-3068
Journal homepage: http://www.journal.acse.science/index.php/ajce/about

Original Article

Carbonized typha grass for the adsorptive removal of alizarin red S from aqueous solution

Musa Sani[a] and Abdullahi Muhammad Ayuba[a]*

[a]*Department of Pure and Industrial Chemistry, Faculty of Physical Sciences, Bayero University, Kano, Nigeria*

ARTICLE INFO

Article history:
Received 29 September 2022
Revised 13 December 2023
Accepted 31 December 2023

Keywords:
Adsorption;
Kinetics;
Thermodynamics;
Equilibrium;
T. latifolia

ABSTRACT

Adsorption of anionic dye Alizarin red S (ARS) on carbonized typha grass (CRB-TG) was studied in an equilibrium batch process. Effects of contact time, initial dye concentration, adsorbent dose, pH, and temperature on the ARS removal were tested. The adsorbent was characterized by scanning electron microscopy (SEM), Fourier transform infrared spectroscopy (FTIR) and point of zero charge (PZC) methods. Equilibrium data were mathematically modelled using the Langmuir, Freundlich, Temkin and Dubinin Radushkevich (D-R) models. Kinetic of adsorption was determined by pseudo first-order, pseudo-second-order Elovich and Intraparticle diffusion models. The thermodynamics quantities of the adsorption process including ΔS (56.983J/molK), ΔH (10.909kJ/mol) and ΔG (-6.359 to -7.499kJ/mol) were calculated from Van't Hoff plot. An optimum equilibrium removal of the anionic dye was obtained at a pH of 6, contact time of 60 minutes, low adsorbent dosage and moderate temperature. The rapid ARS adsorption verified the efficiency of CRB-TG with a maximum adsorption capacity of 46.296mg/g. The data generated were best described by pseudo-second-order kinetic model and the adsorption isotherm was favoured by Freundlich compared to other models tested. The thermodynamics parameters indicate the process to be rapid, feasible and spontaneous. The obtained results show that carbonized typha grass can be used as a readily available, low cost, eco-friendly adsorbent for the removal of anionic dyes from waste water with improved efficacy as an outstanding alternative to the commercially available adsorbents.

1. Introduction

Dyes are commonly used in different industrial applications such as textile, paint, paper, plastics, pharmaceutical and food [1]. Wastewater, from these dye using industries is one of the major environmental hitches resulting to the characteristics of wastewater such as strong colour, high chemical oxygen demand (COD) derived from additives and surfactants with a low biodegradability property [2]. These dyes are the most problematic pollutants of industrial wastewaters [3]. Ordinarily, the wastewater contains dye concentrations ranging from 10 to 200 mg L^{-1} [4]. Hence, a treatment process should be piloted before the wastewater containing dyes is releases to the water environment. Currently, several processes for the treatment of the wastewater containing dyes are available. In terms of cost and efficiency, the adsorption process is the most appropriate method for treating wastewater containing dyes, especially at low concentrations. The success of treating wastewater containing dyes using the adsorption process is highly dependent on the adsorption capacity of the adsorbent under study [5].

A number of studies have focused on different adsorbents for contaminants removal including, carbon nanotubes, activated carbon, clays, metal oxides, minerals and resins [6]. Activated carbon is the most popular

* *Corresponding author*. Tel.: +2348062771500
E-mail address: ayubaabdullahi@buk.edu.ng
http://dx.doi.org/ 10.5281/zenodo.7679064

adsorbent and has been recognised as one of the best available options in the removal of pollutants from wastewater. Due to its large surface area and controllable pore structure, activated carbon display extremely high adsorption efficiency for many adsorbates [7].

The purpose of this study is to examine the effectiveness of carbonized typha grass (*T. Latifolia)* towards the removal of ARS (Fig. 1) from aqueous solution through the use of batch experiments. This was investigated by varying the effects of operating conditions including contact time, adsorbent dose, initial concentration, pH and temperature.

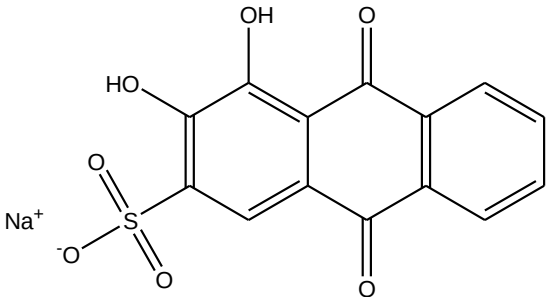

Fig. 1. Alizarin red S (3,4-dihydroxy-9,10-dioxo-9,10-dihydroanthracene-2-sulfonic acid sodium salt)

2. Materials and Methods

2.1 Sample collection and preparations

The typha grass was obtained from Marma town, Guri local government area of Jigawa State, Nigeria. The sample was first washed with tap water then distilled water to remove the impurities [8]. The sample was air-dried then oven dried at 105^0C. The dried sample was carbonized in a muffle furnace at a temperature of 400^0C for 1 hour [9]. The carbonized sample was pulverized and passed through a 2mm sieve and labelled as CRB-TG for further use.

2.2 Preparation of dye solution

The stock solution (Alizarin Red S (ARS) dye) was prepared by dissolving exactly 1g of the dye into a 1L to produce 1000 mg/L using distilled water. The experimental solutions of chosen concentration were prepared accordingly by diluting the stock solution with distilled water. The concentration of the un-adsorbed ARS dye was measured at λmax = 424.89 nm using UV-Visible Spectrometer (Perkin Elmer, Lambda 35).

2.3 Characterization of the adsorbent

2.3.1 Scanning electron microscopy (SEM)

The surface morphological change of the adsorbent sample was investigated using Scanning Electron Microscope (Phenom World Eindhoven). Scanned micrographs of adsorbents before and after ARS adsorption were taken at an accelerating voltage of 15.00 kV and x500 magnification.

2.3.2 Fourier transform infrared spectroscopy (FTIR)

FTIR analysis of adsorbent before and after ARS adsorption was carried out using Cary 630 Fourier Transform Infrared Spectrophotometer Agilent Technology. The analysis was done by scanning the sample through a wave number range of 650 – 4000 cm^{-1}; 32 scans at $8cm^{-1}$ resolution.

2.3.3 Determination of point of zero charge

Points of zero charge (PZCs) are pH values at which the surface charge components become equal to 0 under given conditions of temperature, applied pressure, and aqueous solution composition [10]. The PZC provides important information about dye adsorption mechanisms. Basically, there are three methods for the determination of point of zero charge namely; (i) Salt addition method (ii) Zeta potential method and (iii) Ion adsorption method

Salt Addition Method was employed in this work. PZC values for adsorbents were determined in 0.1 M $NaNO_3$ solution at 303-333K. In this method, 0.2 g of sample was added to 40.0 mL of 0.1 M $NaNO_3$ solution. The pH of the suspension was then adjusted with 0.1 M HCl and 0.1 M NaOH using pH-meter (MP 220) to obtain an initial pH value of 2, 4, 6, 7, 8, 10 and 12. Each flask then was vigorously agitated in a shaker bath for 24 h. After settling, the final pH of each suspension was measured very carefully. The ΔpH (the difference between final and initial pH) values were then plotted against the initial pH values [11]. The initial pH at which ΔpH is zero was taken to be the PZC [12].

2.4 Batch adsorption experiment

Batch experiments were carried out to determine the optimum conditions for the equilibrium adsorption of ARS onto carbonized typha grass (CRB-TG). The results attained after the optimization experiments were used to conduct the batch adsorption experiments. Each of these systems were separately run in a 250 cm^3 conical flask differently at 30, 40, 50^0C respectively. The conical flasks were covered during the equilibration period and placed on a temperature-controlled tightly Innova 4000 incubator shaker for the earlier reported period. After reaching adsorption equilibrium, the content was filtered through Whatman No 1 filter paper. The filtrate was analysed using Perkin-Elmer UV-visible spectrophotometer at maximum absorbance wavelength of 424.89nm. The extent of adsorption was calculated using equations (1) and (2)

respectively.

Adsorption Capacity (q_e) = $\frac{(Co-Ce)x\,V}{m}$ (1)

% adsorption = ($\frac{Co-Ce}{Co}$) x 100 (2)

Where qe is the adsorption capacity (mg/g), *Co* and *Ce* are the initial and final equilibrium concentration (mg/l) of Alizarin Red S in solution, V is the volume of Alizarin Red S in solution (L), and *m* is the mass (g) of the adsorbent.

3. Results and Discussion

3.1 Fourier transform infrared spectroscopy (FT-IR)

The FTIR spectra of the adsorbent CRB-TG before and after adsorption of ARS are presented in Figure 2. Peaks were observed at 3320, 2914 1607, 1547 and 1104 cm^{-1} in CRB-TG before adsorption, which were attributed to O-H stretching, C-H stretching, C=O stretching and C=C stretching respectively [13, 14]. The free O–H stretch for CRB-TG appeared before adsorption at 3320cm^{-1} (Table 1). After loading CRB-TG with ARS there was an observable shift in the vibration frequency of the free O–H stretch. These shifts in the vibration frequencies might be due to binding of ARS molecules onto the surface of the adsorbents [15]. However, The FTIR spectrum after adsorption also shows other shifted peak positions indicating interactions between the adsorbent (CRB-TG) and the dye (ARS). Furthermore, the presence of hydroxyl group and carbonyl group is attributed to the presence of carboxylic acids group present in the CRB-TG adsorbent. The hydroxyl, carboxyl and carboxylic acid are important adsorption sites [16].

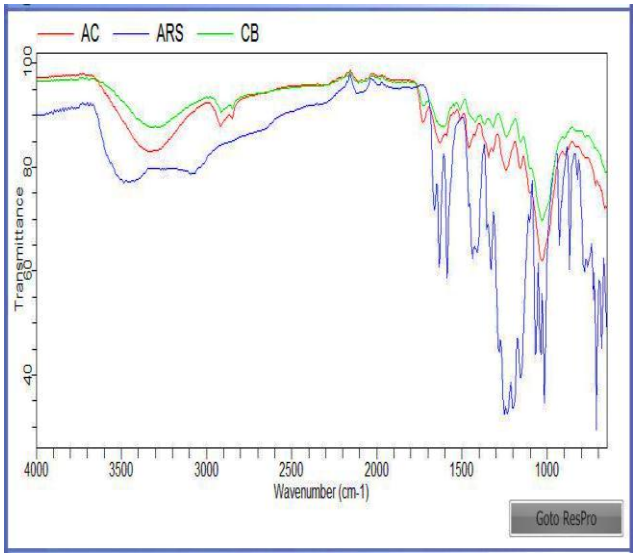

Fig. 2. Overlaid FTIR spectrum ARS and CRB before and after adsorption

Table 1. Different functional group recognized before and after adsorption of ARS onto CRB-TG

Functional Group	Absorption range (cm^{-1})	Before absorption (cm^{-1})	After absorption onto ARS (cm^{-1})	Difference (cm^{-1})
OH stretch	3700-2500	3309	3335	26
C-H stretch	3000-2840	2914	2918	4
C=O stretch	1710-1580	1607	1629	12
C≡C stretch				
C-O stretch	1675-1550	1547	1510	37
	1080-1300	1104	1104	0

3.2 Scanning electron microscopy (SEM)

The SEM micrographs of the adsorbents before and after adsorption of ARS are presented in Fig 3. However, the machine was operated at an accelerating voltage of 15.00 kV and at magnification between 300-1000, but that of x500 were chosen. The scanned micrographs of CRB-TG before adsorption (Fig. 3a) shows a moderately rough surface which is characterized with defects made of cracks and holes and it might be due to the existence of adhering particles which may be dust or other impurities [17]. But when compared with that of CRB-TG after adsorption of ARS, a smooth surface was observed with the surface defects earlier observed disappearing due to the coverage of ARS on CRB-TG surface.

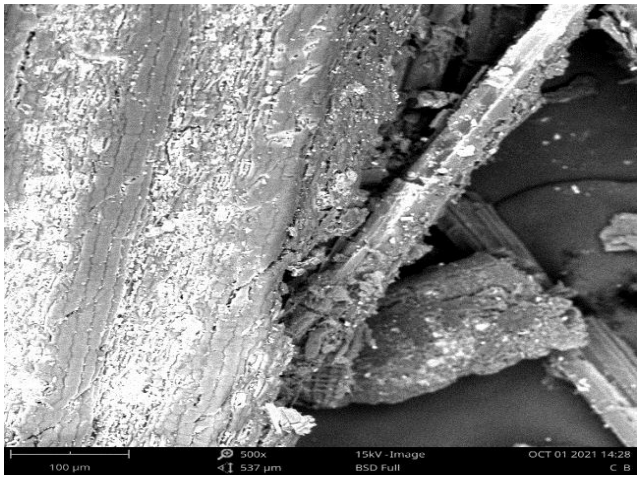

(a)

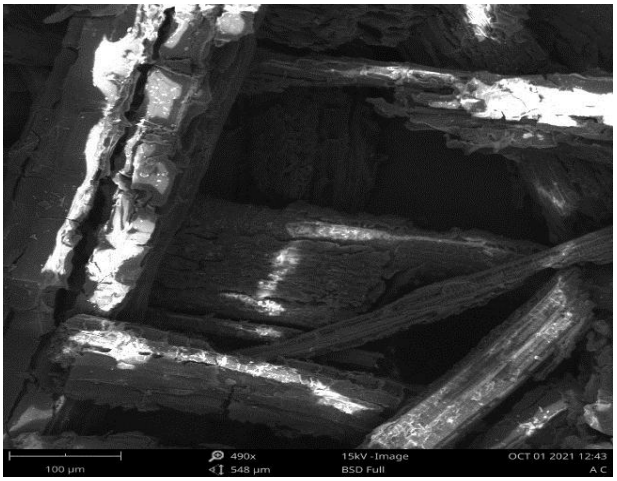

(b)

Fig. 3**.** SEM Micrograph of CRB-TG (a) before and (b) after adsorption of ARS

3.3 Determination of point of zero charge

The points of zero charge (PZCs) result for CRB-TG adsorbent is presented in Fig. 4.

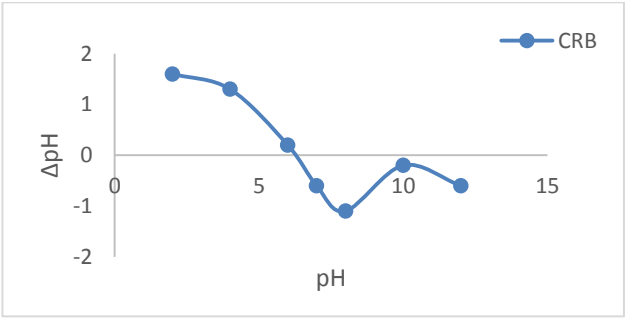

Fig. 4. Point of Zero Charge (PZC) of CRB-TG

The PZC studied was found to be 6.02, which indicate the presence of charge balance in the acidic medium, the region among the equilibrated ions in an aqueous solution. Moreover, substrates with low PZC values show the highest tendency to treat effluents contaminated with cations, while substrates with high PZC values would be more appropriate to capture anions. The magnitude of the surface charge depends on the abundance and types of functional groups present, and on the pH of the solution [18].

3.4 Batch adsorption

(a) Effect of contact time

Figure 5(a) depicts contact time effect which is one of the important parameters affecting the adsorption efficiency. In this experiment, to obtain better adsorption efficiency, 0.02g of CRB-TG was added to 20cm^3 mixture solutions respectively, and then the vortex was rotated at different time intervals. The adsorption equilibrium was reached at 60mins of the vortex, and the removal rate is higher than 80% while the adsorption capacity was found to be 9.53 mgg^{-1}. However, the removal rate of adsorbate was rapid initially, but gradually decreases with time until it reaches equilibrium. This can be due to the fact that a large number of vacant surface sites are available for adsorption at the initial stage, and after a lapse of time, the remaining vacant surface sites are not easily occupied due to repulsive forces between the solute molecules on the solid and bulk phases. Similar findings were reported by other authors [19].

(b) Effect of adsorbent dosage

Figure 5(b) represents the profile diagram of the doses for CRB-TG used for the removal of ARS dye. Different adsorbent dosages in the range of 0.02g - 0.2g were added to ARS solution with the initial concentration of 50mg L^{-1}. Adsorption increases with increase in the adsorbent dose until when the optimum was reached; the removal efficiency of ARS was gradually increased. Therefore, in this experiment 0.02g was chosen as the optimal dosage, and the adsorption capacity was fond to be 46.78 mgg^{-1} [20].

(c) Effect of initial concentration

Figure 5(c) displays the plot showing the effect of initial dye concentration on the adsorption of ARS onto CRB-TG. It was detected that the total mass of ARS adsorbed per gram of the adsorbent increased with increasing concentration. At low concentration, the available driving force for transfer of ARS onto CRB-TG particles is low, while at high concentration, there is a corresponding increase in the driving force, thereby improving the interaction between the ARS dye in the aqueous phase and the active sites of the adsorbent [21].

(d) Effect of pH

Figure 5d shows the effect of pH on the adsorption of ARS onto CRB-TG. Acidic pH had an effective influence on the acceptance of ARS increasing the pH from 2 toward 10, the uptake capacity of the adsorbent increased up to pH 6. The maximum adsorption of ARS dye by CRB-TG happened at pH 6, leading to 48.74mg/g. This outcome can be due to the change in surface charge of the activated carbon in respect to solution pH [22]. However, it was observed that the lowest uptake capacity was determined at pH 4 in the acidic range of experimentation [23].

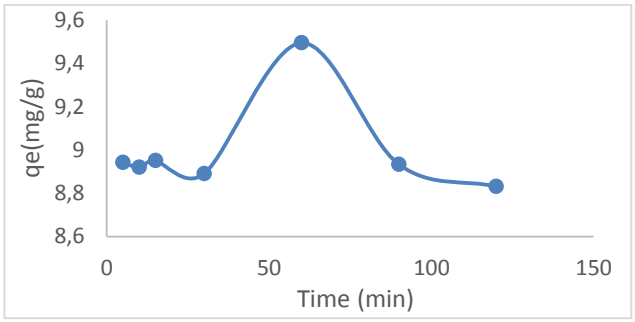

(a)

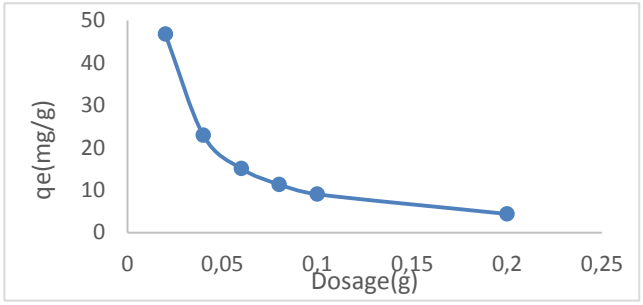

(b)

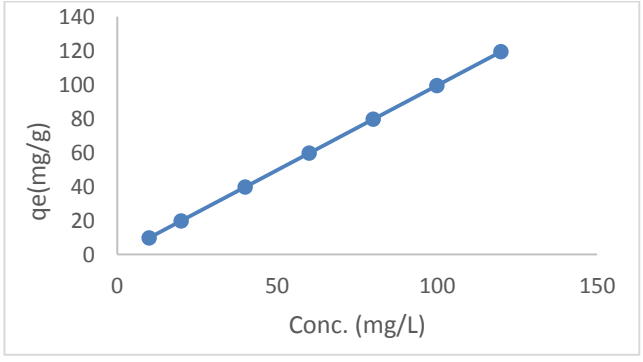

(c)

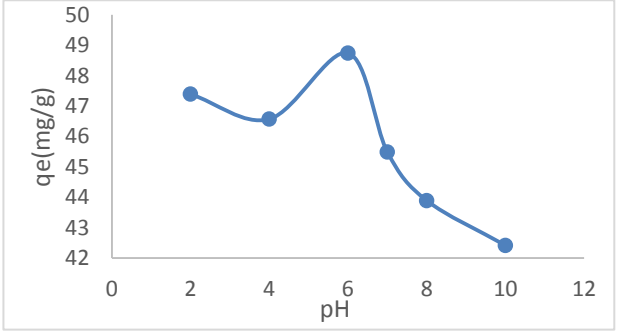

(d)

Fig. 5**.** Effect of (a) contact time (b) Adsorbent Dosage (c) Initial Concentration (d) pH on the Adsorption of ARS onto CRB-TG

3.5 Adsorption kinetics

Kinetic studies are useful to provide information about dye uptake rate, which gives important information for designing and modelling the adsorption processes [24]. Therefore, the removal rate and equilibrium time remain very substantial to study the adsorption mechanism [20]. The data generated during batch adsorption experiments when samples were withdrawn at 10 minutes' interval for a maximum period of 120 minutes was subjected to different kinetic models. This is with an aim of possibly establishing the mechanism of the interaction of the dye with the surface of the adsorbent (CRB-TG). The following models were tested, reported and discussed.

(a) The pseudo first-order equation

The pseudo first-order equation [25] is generally expressed as follows:

$$\frac{dq_t}{dt} = k_1(q_e - q_t) \qquad (3)$$

Where: q_e and q_t are the adsorption capacity at equilibrium and at time t, respectively ($mg.g^{-1}$), k_1 is the rate constant of pseudo first-order adsorption ($l.min^{-1}$). After integration and applying boundary conditions t = 0 to t = t and q_t = 0 to q_t = q_t, the integrated form of Eq. (3) becomes:

$$\log(q_e - q_t) = \log(q_e) - \frac{k_1}{2.303}t \qquad (4)$$

The values of log (q_e - q_t) were linearly correlated with t. The plot of log (q_e - q_t) vs. t should give a linear relationship from which k_1 and q_e can be determined from the slope and intercept of the plot respectively (Fig. 6a).

(b) The pseudo second-order equation

Kinetic rate equation for the pseudo second-order adsorption is expressed as:

$$\frac{dq_t}{dt} = k_2(q_e - q_t)^2 \qquad (5)$$

The pseudo second-order adsorption rate constant is k_2 ($g.mg^{-1}min^{-1}$). For the boundary conditions t = 0 to t = t and q_t = 0 to q_t = q_t, the integrated form of Eq. (5) becomes:

$$\frac{1}{(q_e - q_t)} = \frac{1}{q_e} + k_2 \qquad (6)$$

Equation (6) rearranged to obtain Eq. (7), a linear form:

$$\frac{t}{q_t} = \frac{1}{k_2 q_e^2} + \frac{1}{q_e}(t) \qquad (7)$$

The initial adsorption rate, h ($mg.g^{-1}min^{-1}$) is;

$$h = k_2 q_e^2 \qquad (8)$$

Then equation (8) becomes

$$\left(\frac{t}{q_t}\right) = \frac{1}{h} + \frac{1}{q_e}(t) \qquad (9)$$

The plot of (t/q_t) against t of Eq. (9) gives a linear relationship from which k_2 and q_e can be obtained from the

intercept and slope of the plot respectively (Fig. 6b).

(c) Elovich Equation

The Elovich kinetic model is defined by the following relation [26].

$$q_t = {}^{1}/_{\beta}\ln(\alpha\beta) + \left({}^{1}/_{\beta}\right) lnt \qquad (10)$$

This model gives useful information on the extent of both surface activity and activation energy for adsorption process. The parameters *(α)* and *(β)* was calculated from the slope and intercept of the linear plot of qt versus ln (t) (Fig. 6c).

(d) Intraparticle Diffusion Equation

The slowest step in an adsorption process is usually taken as the rate determining step. This step is often attributed to pore and intra particle diffusion. Since pseudo first and pseudo second order models cannot provide information on effect of intra particle diffusion in adsorption, intra particle diffusion model can be used. Possibility of involvement of intra particle diffusion model as the sole mechanism was investigated according to Weber–Morris equation (11) [2, 27].

$$q_t = C + K_{int} t^{1_2} \qquad (11)$$

Where the constant k_{int} (mg/g $min^{0.5}$) is the intra particle diffusion rate and *C* is the boundary layer thickness. If the rate-limiting step is only due to the intra particle diffusion, then *qt* versus $t_{1/2}$ will be linear and the plot passes through the origin (Fig. 6d).

Table 2. Kinetic models parameters for the adsorption of ARS onto CRB-TG

Kinetic Models	**Parameters**			
Pseudo-first order	qe_{Cal} (mg/g)	qe_{Exp} (mg/g)	k_1 (min^{-1})	R^2
	46.446	0.258	0.009	0.003
Pseudo-second order	qe_{Cal} (mg/g)	qe_{Exp} (mg/g)	k_2 (min^{-1})	R^2
	46.446	46.296	0.583	0.999
Elovich		B	A	R^2
		7.122	5.247	0.408
Intraparticle diffusion		k_3	C	R^2
		0.056	45.91	0.355

Table 2 shows the parameters obtained from the tested kinetic models for the adsorption of ARS onto CRB-TG. The pseudo-second-order kinetic model support the experimental data relatively quite well; the correlation coefficients values, R^2, are all close to unity, the theoretical and experimental uptakes are well in good agreement. This gives the applicability of the second-order kinetic model to describe the adsorption process of ARS onto the adsorbent.

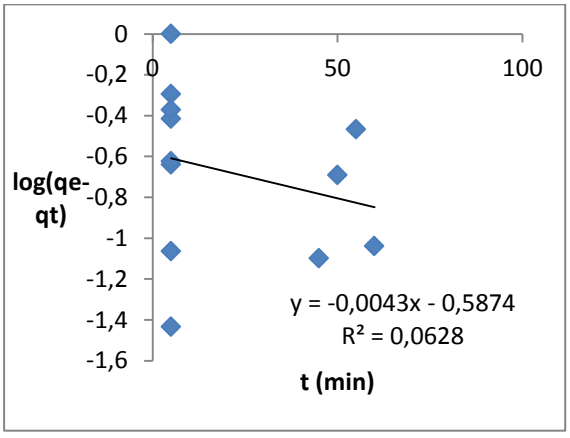

(a)

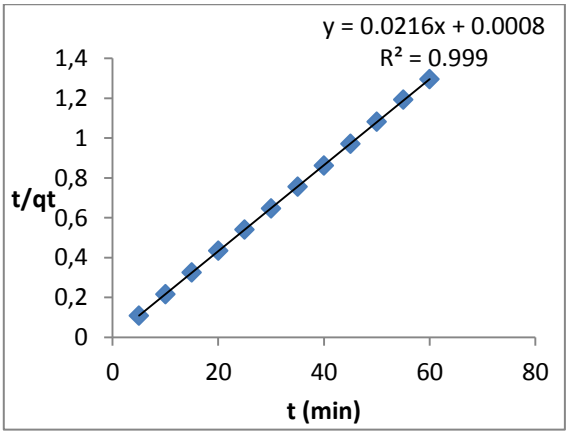

(b)

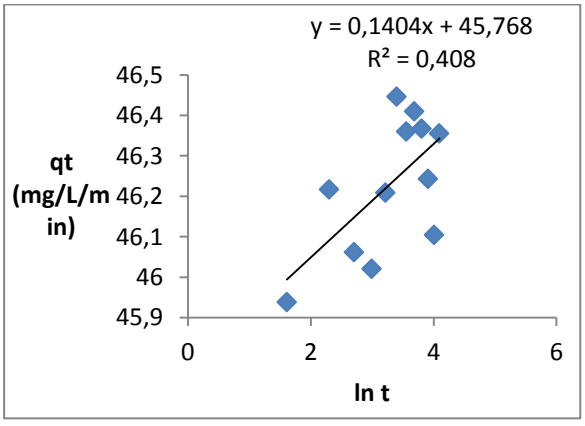

(c)

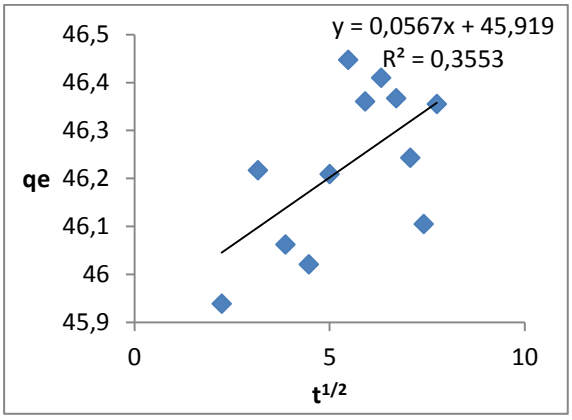

(d)

Fig. 6. Adsorption Kinetics of (a) first order (b) second order (c) Temkin (d) Intraparticle of ARS onto CRB-TG

3.6 Adsorption isotherms

The relationship between the equilibrium concentration of the adsorbate in the liquid phase and in the solid phase adsorbent was subjected to four different adsorption isotherm equations. More importantly, to determine which of the isotherms best describes the adsorption process. Experimental data were substituted into the equations and appropriate graphs, constants and other variables were generated for each of the following equations:

(a) Langmuir isotherm

This report quantitatively the formation of a monolayer adsorbate on the surface of the adsorbent, without further adsorption takes place. So, the Langmuir stands in the place of equilibrium distribution of dyes between the solid and liquid phases [28].

Langmuir signified the following equations:

$$q_e = \frac{Q_{OK_lC_e}}{1 + K_lC_e} \qquad (12)$$

Langmuir adsorption parameters were obtained by converting the Langmuir equation (12) into linear form.

$$\frac{1}{q_e} = \frac{1}{Q_o} + \frac{1}{Q_oK_lC_e} \qquad (13)$$

Where: C_e= the equilibrium concentration of adsorbate (mg.l^{-1}), q_e = the amount of dye adsorbed per gram of the adsorbent at equilibrium (mg.g^{-1}), Q_o= maximum monolayer coverage capacity (mg.g-1), K_l= Langmuir isotherm constant (L.mg^{-1}).

The values of q_{max} and K_l were computed from the slope and intercept of the Langmuir plot of $\frac{1}{qe}$ versus $\frac{1}{Ce}$ (Fig. 7a) [29]. The essential features of the Langmuir isotherm may be expressed in terms of equilibrium parameter R_L, which is a dimensionless constant referred to as separation factor or equilibrium parameter [30].

$$R_L = \frac{1}{(1 + K_lC_o)} \qquad (14)$$

Where: Co = initial concentration, K_l = the constant related to the energy of adsorption (Langmuir constant), R_L value indicates the adsorption nature to be either unfavourable if R_L>1, linear if R_L=1, favourable if 0<R_L<1 and irreversible if R_L= 0.

(b) Freundlich isotherm

This is commonly used to describe the adsorption characteristics for the heterogeneous surface [31]. These data always fit the equation proposed by Freundlich:

$$Q_e = K_fC_e^{1/n} \qquad (15)$$

Where K_f = Freundlich isotherm constant (mg.g^{-1}), n = adsorption intensity, Ce = the equilibrium concentration of adsorbate (mg.L^{-1}), Qe = the amount of the ARS adsorbed per gram of the adsorbent at equilibrium (mg.g^{-1}). Changing equation (15) to linear form, give:

$$LogQ_e = logK_f + \frac{1}{n}logC_e \qquad (16)$$

The plotting of ARS molecule adsorbed logqe by CRB-TG against the equilibrium concentration of ARS molecule logCe in solution (Fig. 7b) gives the equilibrium isotherm and the values of the parameters calculated are tabulated in table 3.

(c) Temkin isotherm

This is categorised by binding energies which is uniform distribution up to the climax of binding energy [32, 33]. The linear equation of this isotherm is represented in Equation. (17):

$q_e = B_T lnC_e + B_T lnK_T$ (17)

$B_T = RT/b_T$ (18)

Figure 7(c) presents the Temkin model plots for the ARS adsorption onto CRB-TG. From Table 3, the B_T (energy of adsorption) value was found to be 36.188 while A_T (equilibrium binding energy) value is 0.934 L mg^{-1}. Therefore, adsorption rate of ARS molecules is bonded to the sites of CRB-TG as indicated in table 3.

(d) Dubinin-Radushkevich (D-R)

Dubinin–Radushkevich isotherm is an empirical model initially conceived for the adsorption of subcritical vapours onto micro pore solids following a pore filling mechanism [34]. The linear form of Dubinin-Radushkevich (D-R) isotherm model is given by equation (19)

$lnqe = lnqm - \beta\varepsilon^2$ (19)

$\varepsilon = RTln\,[1 + 1/Ce]$ (20)

$E = 1/\sqrt{2\beta}$ (21)

The mean free energy (E) obtained from Dubinin-Rudushkevich (D-R) model provides information about

chemical or physical properties of the adsorption process [35]. A plot of lnqe versus ε^2 is as presented in Fig 7(d). The D-R correlation coefficient is the lowest (R^2) as observed from table 3 in comparison with all the studied isotherms. Thus, the D-R model exhibited less fit with the experimental data. The E value was less than 8 kJ mol^{-1} implying that the adsorption process is controlled by physical forces [23].

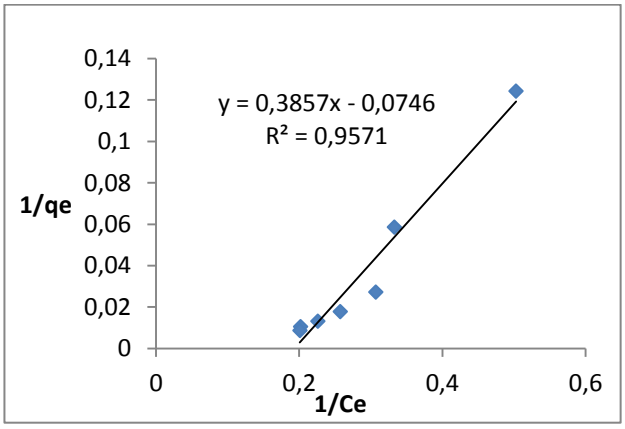

(a)

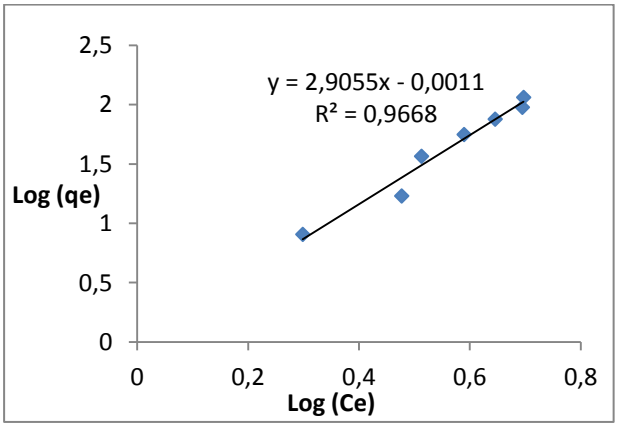

(b)

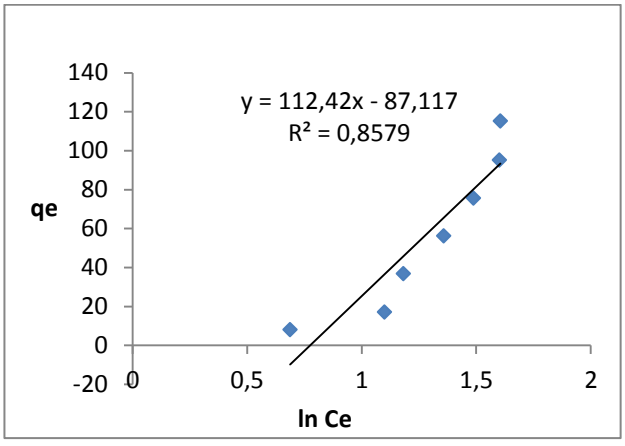

(c)

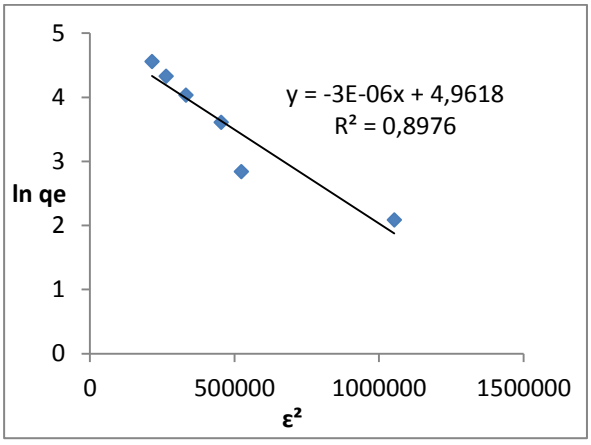

(d)

Fig. 7. Adsorption isotherms plots Langmuir (a) Freundlich (b) Temkin (c) Dubinin-Radush-kevich for the adsorption of ARS onto CRB-TG.

Table 3. Adsorption isotherm parameters for ARS adsorption onto CRB-TG

Parameter	Alizarin Red S
Langmuir	
Q_O(mg/g)	-4.1034
K_L(L/mg)	-0.1459
R_L	-0.1429
R^2	0.603
Freundlich	
1/n	2.046
N	0.4770
K_F	0.0155
R^2	0.966
Temkin	
A_T	0.2201
B_T	11.153
B	225.82
R^2	0.920
Dubinin-Radushkevich	
q_m(mg/g)	1107.54
K_{dr}(mol^2/kJ^2)	2.0×10^{-5}
E(kJ/mol)	1.0×10^{-1}
R^2	0.810

3.7 Thermodynamic studies

The influence of temperature on Alizarin Red S adsorption onto CRB-TG was determined by changing the temperature from 303 - 323K and by keeping all factors (contact time, pH, adsorbent dose, agitation speed and initial ARS concentrations) constant at optimized values. The thermodynamic parameters such as changes in Gibb's free energy (ΔG), enthalpy (ΔH) and entropy (ΔS) give

expedient opinion about the feasibility and the spontaneous nature of the adsorption process using equations (22), (23) and (24):

$\Delta G = -RT\ln K_L$ (22)

$\Delta G = \Delta H - T\Delta S$ (23)

Where R is the gas constant (8.314 J/molK), T is the absolute temperature (K), and K_L is the thermodynamic equilibrium constant.

From equations (22) and (23) we get the equation (24)

$$\ln K_L = -\frac{\Delta H}{RT} + \frac{\Delta S}{R} \quad (24)$$

The plot of $\ln K_L$ (L/mol) versus 1/T (Van't Hoff) was constructed and ΔH and ΔS values were calculated from the slope and intercept of the plot, and K_L is equal to qe/Ce obtained at different temperatures [36].

Table 4. Thermodynamic parameters for the adsorption of Alizarin Red S onto CRB-TG

T (K)	K_L	ΔG (kJ/mol)	ΔH (kJ/mol)	ΔS (J/mol.K)
303	12.482	-6.359		
313	14.283	-6.919	10.909	56.983
323	16.322	-7.499		

The negative value of the Gibbs free energy (ΔG) in table 4 suggests that the ARS removal using CRB-TG is thermodynamically feasible and spontaneous. The increase in the negative value at elevated temperatures indicates that the adsorbate uptake by CRB-TG is improved at higher temperatures in the studied range. The positive value of the enthalpy change (ΔH) implies the endothermic nature of the adsorption process. The extent of enthalpy change (ΔH) may provide an insight about the kind of adsorption process involved. If the value of ΔH is greater than 80 kJ/mol, the process is considered chemisorption which involves chemical bonding between the adsorbate and adsorbent surface. On the other hand, when ΔH is lower than 80 kJ/mol, it signifies the adsorption process is physisorption which fully describe the process under investigation [37].

4. Conclusion

The results of this study showed that the carbonized typha grass is a good adsorbent for the removal of anionic dye (ARS) from aqueous solution. The adsorbent was investigated on the effect of contact time, adsorbent dose, initial ARS concentration, pH and temperature which are greatly reliant on the efficiency of adsorption. The attained adsorption kinetics fitted well with pseudo-second order model, and the adsorption isotherms was best described by the Freundlich isotherm model. The adsorption process was qualified to be spontaneous and feasible based on the thermodynamic parameters calculated including enthalpy, entropy and Gibb's free energy. The results suggested that CRB-TG had the potential to become a favourable adsorbent for removal of anionic dye such as Alizarin Red S present in the wastewater.

Acknowledgements

The authors wish to thank Mr. Musa Garba Beli and Mr Muhammed Buhari Umar of Central Laboratory Complex, Bayero University, Kano, Nigeria for the assistance rendered during the characterization of the adsorbent.

Conflict of Interest

The authors declare that they have no conflict of interest

Nomenclature and Notations

ARS: Alizarin red S
CRB-TG: Carbonized typha grass
SEM: Scanning electron microscopy
FTIR: Fourier transforms infrared
PZC: Point of zero charge
ΔpH: The difference between final and initial pH
ΔH: Enthalpy change of adsorption
ΔS: Entropy change of adsorption
ΔG: Gibb's free energy change of adsorption

References

[1] Ayuba, A. M and Idoko, B. (2020) Kinetic, equilibrium and thermodynamic studies on the adsorption of crystal violet dye from aqueous solution using activated cowpea (*Vigna Unguiculata)* husk, Applied Journal of Environmental Engineering Sciences, 6(2), 182-195. https://doi.org/10.48422/IMIST.PRSM/ajees-v6i2.20984.

[2] Ayuba, A. M. and Idoko B. (2021) Cowpea husk adsorbent for the removal of crystal violet dye from aqueous solution, Arabian Journal of Chemical and Environmental Research 08(01), 114–132.

[3] Sharma, S. K (2015) Green Chemistry for Dyes Removal from Waste Water Scrivener Publishing Cummings Center, Suite 100 Cummings Center, Suite 541J Beverly, MA 01915-6106 Pp. 142-180 100.

[4] Kumar, P.S., Ramalingam, S., Senthamarai, C., Niranjanaa, M., Vijayalakshmi, P., Sivanesan, S., (2010). Adsorption of dye from aqueous solution by cashew nut shell: studies on equilibrium isotherm, kinetics and thermodynamics of interactions. Desalination, 261, 52–60. https://doi.org/10.1016/j.desal.2010.05.032.

[5] Putro, Jindrayani Nyoo, Yi-Hsu, Ju, Felycia Edi Soetaredjo, Shella Permatasari Santoso, Suryadi Ismadji (2021). Biosorption of dyes, *Green Chemistry and Water Remediation.* 5 (3), 67-84 https://doi.org/10.1016/B978-0-12-817742-6.00004-9.

[6] Umar, Yunusa. Abdulrahman, Ibrahim Kubo, Yusuf Abdullahi, Tahir Abdullahi and Musa Husaini (2021). Hexavalent chromium removal from simulated wastewater using biomass-based activated carbon: kinetics, mechanism, thermodynamics and regeneration studies, Algerian Journal of Engineering and Technology 04, 030–044. http://dx.doi.org/10.5281/zenodo.4542410.

[7] Bello, O. S. Adegoke, K. A. Olaniyan, A. A. Abdulazeez, H. (2013) Dye adsorption using biomass wastes and natural adsorbents: overview and future prospects. Desalination and Water Treatment, 53(5), 1292-1315. https://doi.org/10.1080/19443994.2013.862028.

[8] Nwosu, F.O., Adekola, F.A., Salami, A.O., (2017). Adsorption of N-nitrophenol (PNP) Using Pilli nut shell action. Pak. J. Anal. Environ. Chem. 18 (1), 69. https://doi.org/10.21743/pjaec/2017.06.07.

[9] Adeniyi, Adewale George and Joshua O. Ighalo (2019) Biosorption of pollutants by plant leaves: An empirical review, Journal of Environmental Chemical Engineering 7(3), 103100. https://doi.org/10.1016/j.jece.2019.103100.

[10] Sposito, G. (2008). The chemistry of soils, 2nd edn. Oxford University Press, New York

[11] Mahmoud, A.E.D. Fawzy, M. Radwan, A. (2016) Optimization of cadmium (Cd^{2+}) removal from aqueous solutions by novel biosorbent, Int. J. Phytoremed. 18 (6), 619–625. https://doi.org/10.1080/15226514.2015.1086305.

[12] Bakatula, E. N. Richard, Dominique, Neculita, Carmen Mihaela Zagury, Gerald J. (2018) Determination of point of zero charge of natural organic materials, Environmental Science and Pollution Research, 25, 7823-7833. https://doi.org/10.1007/s11356-017-1115-7.

[13] Ali, H. Mladenka, N. Mihajlović, I. (2019) Sorption of carbendazim and linuron from aqueous solutions with activated carbon produced from spent coffee grounds: Equilibrium, kinetic and thermodynamic approach, Journal of Environmental Science and Health, Part B, 54(4), 226-236. https://doi.org/10.1080/03601234.2018.1550307.

[14] Werkneh, A.A., Habtu, N.G. and Beyene, H.D. (2015). Removal of Hexavalent Chromium from Tannery Wastewater using Activated Carbon Primed from Sugarcane Bagasse: Adsorption/Desorption Studies. American Journal of Applied Chemistry 2(6), 128-135. https://doi.org/10.11648/J.AJAC.20140206.16.

[15] Babalola, J.O. Olowoyo, J.O. Durojaiye, A.O. Olatunde, A.M. Unuabonah, E.I. Omorogie, M.O (2016) Understanding the removal and regeneration potentials of biogenic wastes for toxic metals and organic dyes. Journal of Taiwan Inst Chem Eng 58, 490–499. https://doi.org/10.1016/j.jtice.2015.07.003.

[16] Itodo, U., Usman A. and Ugboaja, C. (2011). A Rate Study of Received and Derived Activated Carbon and Pseudo Constants for Methyl Red Sorption. Journal of Encapsulation and Adsorption Sciences, 1, 57- 64. http://dx.doi.org/10.4236/jeas.2011.14008.

[17] Chowdhury, S. Mishra, R. Saha, P. Kushwaha, P. (2011). Adsorption thermodynamics, kinetics and isosteric heat of adsorption of malachite green onto chemically modified rice husk. Desalination 265, 159–168 doi:10.1016/j.desal.2010.07.047

[18] Mukherjee, A. Zimmerman, A. R. Harris, W. (2011) Surface chemistry variations among a series of laboratory-produced biochars. Geoderma 163(3-4), 247–255. https://doi.org/10.1016/j.geoderma.2011.04.021

[19] Abdus-Salam, N. Adekola, S.K. (2018) Biosorption of Dyes. App.Water Sci., 28-222. https://doi.org/10.1007/s13201-018-0867-7.

[20] Lee, S., Park, J., Kim, S., Kang, S., Cho, J., Jeon, J., Lee, Y., and Seo, D. (2019). Sorption Behavior of Malachite Green onto Pristine Lignin to Evaluate the Possibility as a Dye Adsorbent by Lignin. Applied Biological Chemistry, 62(37), 1-10. https://doi.org/10.1186/s13765-019-0444-2.

[21] Liu, P., Jiang, L., Zhu, L., Guo, J., Wang, A. (2015). Synthesis of covalently crosslinked attapulgite/poly(acrylic acid-co-acrylamide) nanocomposite hydrogels and their evaluation as adsorbent for heavy metal ions. *J. Ind. Eng. Chem.*, 23, 188–193. https://doi.org/10.1016/j.jiec.2014.08.014.

[22] Alam J. B., Dikshit A. K. and Bandopadhyay M. (2000). Efficacy of Adsorbents for 2, 4-D and Atrazine Removal from waste water environment, *Global Nest Journal*, 2(2), 139-148. https://doi.org/10.30955/gnj.000166.

[23] Nwosu, F.O., Adekola, F.A., Salami, A.O., (2017). Adsorption of N-nitrophenol (PNP) Using Pilli nut shell action. Pak. J. Anal. Environ. Chem. 18 (1), 69. https://doi.org/10.21743/pjaec/2017.06.07.

[24] Aharoni, C. and Ungarish, M. (1977). Kinetics of activated chemisorption. Part 2. Theoretical Models. Journal of Chemical Society. Faraday Transaction 1: Physical Chemistry in Condensed Phases, 73, 456-464. https://doi.org/10.1039/F19777300456.

[25] Ayuba, A. M. Ladan, M. Muhammad, A. S. (2020) Thermodynamic and kinetic study of Pb(II) amputation by river sediment. Appl. J. Envir. Eng. Sci. 6(3), 213-226. https://doi.org/10.48422/IMIST.PRSM/ajees-v6i3.22383.

[26] Guo, S., Liang, X., Feng, N., Tian, Q. (2010). Isotherms, kinetics and thermodynamic studies of adsorption of Cu^{2+} from aqueous solutions by Mg^{2+}/K^{+} type orange peel adsorbents. J. Hazard. Material. 174, 756–762. https://doi.org/10.1016/j.jhazmat.2009.09.116.

[27] Weber, WJ, Morris, JC. (1963) Kinetics of adsorption on carbon from solution. Journal of the sanitary engineering division. 89 (2), 31-60. https://doi.org/10.1061/JSEDAI.0000430.

[28] Hall, K. R., Eagleton, L. C., Acrivos, A. and Vermeulen, T. (1966). Pore- and Solid-Diffusion Kinetics in Fixed-Bed Adsorption under Constant-Pattern Conditions, *Industrial & Engineering Chemistry Fundamentals*, 5(2), 212-223. doi: 10.1021/i160018a011.

[29] Langmuir, I. (1918) The adsorption of gases on plane surfaces of glass, mica and platinum, J. Am. Chem. Soc. 40(9), 1362-1403. https://doi.org/10.1021/ja02242a004.

[30] Mckay, G., Blair, H.S. and Gardiner, J.R. (1984). The adsorption of dyes onto chitin in fixed bed column and batch absorbers. *Journal of Applied Polymer Science*, 29(5), 1499-1514. https://doi.org/10.1002/app.1984.070290504.

[31] Hutson, N.D and Yang, R.T (2000) Structural effects on adsorption of atmospheric gases in mixed Li, Ag-X-zeolite, Alche journal 46 (11), 2305-2317. https://doi.org/10.1002/aic.690461121.

[32] Temkin, M.I. and Pyzhev, V. (1940). Kinetics of ammonia synthesis on promoted catalyst. Acta.phys. Chim. *USSR*. 12, 217-222.

[33] Smith, T., Santhi, T., Prasad, A.L., Manonmani, S., (2017). Cucumis Sativus used as adsorbent for the removal of dyes from aqueous solution. Arab. J. Chem. 10, S244–S251. https://doi.org/10.1016/j.arabjc.2012.07.030.

[34] Dubinin, M.M and Radushkevich, L.V. (1947). The equation of the characteristics curve of the activated charcoal. Proc. Acad. Sci. USSR Phys. Chem. Sect. 55:331-337.

[35] Ushakumary, E.R. and Madhu, G. (2014). Removal of cadmium, chromium, copper, lead, and zinc ions by Alisma plantago aquatica. International Journal of Environment and Waste Management 13(1), 75-89. https://dx.doi.org/10.1504/IJEWM.2014.058796.

[36] Sumanjit, K. and Walia, T. P. S (2008). Use of Dairy Sludge for the Removal of Some Basic Dyes. Journal of Environmental Engineering and Science. 7 (5), 433-438. https://doi.org/10.1139/S08-017.

[37] Akar, E. Altinisik, A. Seki, Y. (2013). Using of activated carbon produced from spent tea leaves for the removal of malachite green from aqueous solution. Journal of Ecological Engineering. 52, 19– 27. https://doi.org/10.1016/j.ecoleng.2012.12.032.

Recommended Citation

Sani, M., Ayuba, A. M. (2022). Carbonized typha grass for the adsorptive removal of alizarin red S from aqueous solution. *Algerian Journal of Chemical Engineering*, 02, 10-20. http://dx.doi.org/10. 10.5281/zenodo.7679064